Journal of the Korean Nuclear Society
Volume 24, Number 3, September 1992

Finite Element Analysis of the Neutron Transport Equation in Spherical Geometry

Yong Ill Kim and Jong Kyung Kim
Hanyang University

Soo Dong Suk
Korea Atomic Energy Research Institute

(Received March 25, 1992)

구형에서 중성자 수송방정식의 유한요소법에 의한 해석

김용일 · 김종경
한양대학교

석수동
한국원자력연구소

(1992. 3. 25 접수)

Abstract

The Galerkin formulation of the finite element method is applied to the integral law of the first-order form of the one-group neutron transport equation in one-dimensional spherical geometry. Piecewise linear or quadratic Lagrange polynomials are utilized in the integral law for the angular flux to establish a set of linear algebraic equations.

Numerical analyses are performed for the scalar flux distribution in a heterogeneous sphere as well as for the criticality problem in a uniform sphere. For the criticality problems in the uniform sphere, the results of the finite element method, with the use of continuous finite elements in space and angle, are compared with the exact solutions. In the heterogeneous problem, the scalar flux distribution obtained by using discontinuous angular and spatical finite elements is in good agreement with that from the ANISN code calculation.

요 약

일차원 구에서 유한요소법의 Galerkin formulation이 일차형태의 단일 에너지 중성자 수송방정식의 적분법에 적용되었다. 구분적으로 1차 혹은 2차인 Lagrange 다항식들이 선형대수 방정식들의 집합을 만들기 위해 적분법에 있는 각의존 중성자속(angular flux)에 대하여 활용되었다.

수치해석이 균질구에서의 임계문제와 비균질구에서의 scalar flux 분포에 대해서 행해졌다. 공간과 각에 대하여 연속적인 유한요소를 사용한 균질구에서의 임계문제에 대한 유한요소법의 결과들은 이론적인 해들과 비교되었다. 비균질 문제에서는 각과 공간에 대하여 불연속 유한요소를 사용하여 구한 scalar flux 분포는 ANISN code에 의한 계산결과와 잘 일치하였다.

1. Introduction

The finite element method in both space and angle to the even-parity second-order form of the neutron transport equation has been studied to solve neutronics problems numerically.[1,2,3] Pitkäranta and Silvennoinen[1] applied the finite element method to a general multigroup formalism in spherical geometry. Miller et al.[2] utilized piecewise bilinear or trilinear polynomials in an even-parity functional for the angular flux to establish linear simultaneous sets of algebraic equations. They also demonstrated that the finite element method to problems with anisotropic scattering and material interfaces is applicable. The application of the finite element method to the various neutron transport problems, where standard discrete ordinates method does not applicable, has been successful. Miller et al.[3] demonstrated the disappearance of ray effects, appearing in the presence of highly absorbing media, in finite element calculations, and the convenience of treating hexagonal geometries and curved boundaries through the use of triangular elements. Ukai[4] and Martin and Duderstadt[5] have also investigated the feasibility of applying the finite element method directly to the first-order form (non-self-adjoint) of the neutron transport equation. The theoretical basis of the method has been examined by Ukai when it is applied in space and angle to the generral transport equation with vacuum boundary condition. Martin and Duderstadt examined in detail the application of the finite element method and obtained successful numerical results for the one-dimensional plane geometry application.

The finite element method is to divide the domain under consideration into small elements and the solution is approximated by piecewise polynomials. The expansion coefficients are determined by applying the Galerkin scheme. In the present study, criticality calculations in a uniform sphere are performed by the finite element method combined with finite elements that are continuous in space-angle phase space. Since most practical problems involve spatially strong heterogeneities, the suitability of the finite element method for describing neutron transport in a heterogeneous system is also examined and the result is compared with that from the discrete ordinates method. For such applications, it is essential to utilize finite elements that are discontinuous in both space and angle. In particular, the use of discontinuous angular elements at $\mu=0$ is introduced and the utilization of discontinuous spatial finite elements is developed for the heterogeneous spherical geometry.

2. Integral Law Formulation in Spherical Geometry

Consider the steady state monoenergetic neutron transport equation for a homogeneous sphere on the interval $0\leq r\leq R$ shown in Fig. 1 as

$$\frac{\mu}{r^2}\frac{\partial}{\partial r}\left[r^2\varphi(r,\mu)\right] + \frac{1}{r}\frac{\partial}{\partial \mu}\left[(1-\mu^2)\varphi(r,\mu)\right] + \Sigma_t(r)\varphi(r,\mu)$$

$$= \int_{-1}^{+1} d\mu' \Sigma_s(r,\mu'\rightarrow\mu)\varphi(r,\mu') + S(r,\mu) \ , \qquad (1)$$

where the streaming operator is expressed in conservation form[6]. In Eq.(1) all notations are standard, and the following specified incoming boundary condition can be imposed:

$$\varphi(R,\mu) = \varphi_0(R,\mu) \ , \ \mu<0 \ .$$

To develop the integral law formulation of the neutron transport equation, Eq.(1) is multiplied by an arbitrary function $\psi(r,\mu) \in H_E$, where H_E is energy or Sobolev space[4,5,7], and integrated over the $(r-\mu)$ phase:

$$\int_0^R dr \int_{-1}^{+1} d\mu\, \psi(r,\mu)\mu\frac{\partial r^2\varphi}{\partial r} + \int_0^R dr \int_{-1}^{+1} d\mu\, \psi(r,\mu)\frac{\partial(1-\mu^2)\varphi}{\partial \mu}$$

$$+ \int_0^R dr\, r^2 \int_{-1}^{+1} d\mu\, \psi(r,\mu)\Sigma_t(r)\varphi(r,\mu)$$

$$- \int_0^R dr\, r^2 \int_{-1}^{+1} d\mu\, \psi(r,\mu) \int_{-1}^{+1} d\mu' \Sigma_s(r,\mu'\rightarrow\mu)\varphi(r,\mu')$$

$$= \int_0^R dr\, r^2 \int_{-1}^{+1} d\mu\, \psi(r,\mu)S(r,\mu) \qquad (2)$$

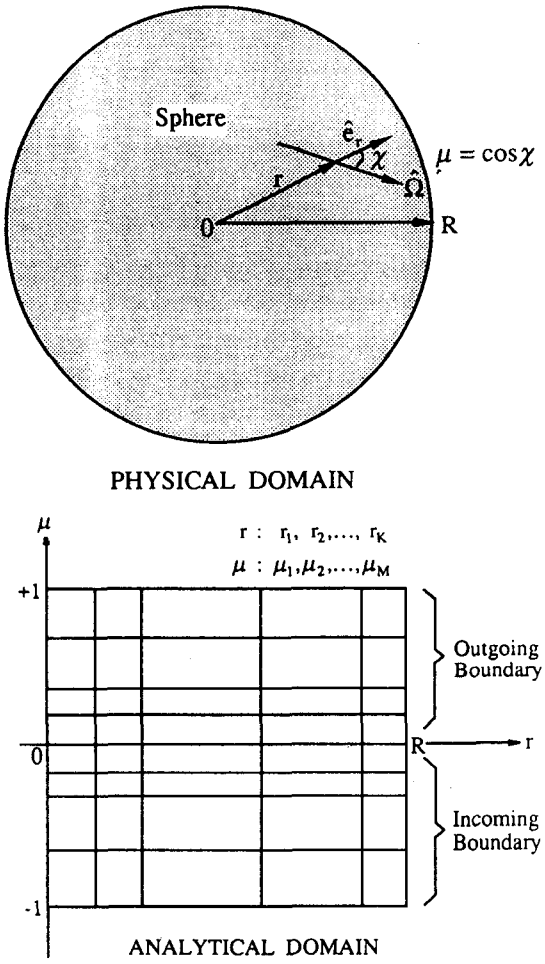

Fig. 1. Physical and Analytical Domains for One-Dimensional Spherical Geometry Application

Integrating the streaming terms, the first and second terms on the left-hand side of Eq.(2), by parts to produce boundary terms, we have

$$\int_0^R dr \int_{-1}^{+1} d\mu\, \psi(r,\mu)\mu \frac{\partial r^2 \varphi}{\partial r} + \int_0^R dr \int_{-1}^{+1} d\mu\, \psi(r,\mu) \frac{\partial (1-\mu^2)\varphi}{\partial \mu}$$

$$= - \int_0^R dr\, r^2 \int_{-1}^{+1} d\mu\, \mu \varphi(r,\mu) \frac{\partial \psi}{\partial r} + \int_{-1}^{+1} d\mu\, \mu \left[r^2 \varphi(r,\mu)\psi(r,\mu) \right]_0^R$$

$$- \int_0^R dr\, r \int_{-1}^{+1} d\mu (1-\mu^2) \varphi(r,\mu) \frac{\partial \psi}{\partial \mu} + \int_0^R dr\, r \left[(1-\mu^2)\varphi(r,\mu)\psi(r,\mu) \right]_{-1}^{+1}$$

$$= - \int_0^R dr\, r^2 \int_{-1}^{+1} d\mu\, \mu \varphi(r,\mu) \frac{\partial \psi}{\partial r} - \int_0^R dr\, r \int_{-1}^{+1} d\mu (1-\mu^2) \varphi(r,\mu) \frac{\partial \psi}{\partial \mu}$$

$$+ R^2 \int_{-1}^{0} d\mu\, \mu \varphi(R,\mu)\psi(R,\mu) + R^2 \int_0^{+1} d\mu\, \mu \varphi(R,\mu)\psi(R,\mu) \quad (3)$$

We can identify the boundary terms in the above equation, the last two terms on the right-hand side of Eq.(3), where the former is known incoming term and the latter is unknown outgoing term. Now the boundary condition at r=R, $\varphi_o(R,\mu)$ for $\mu<0$, can be substituted into Eq.(3). Therefore, Eq.(2) can be rewritten as

$$- \int_0^R dr\, r^2 \int_{-1}^{+1} d\mu\, \mu \varphi(r,\mu) \frac{\partial \psi}{\partial r} - \int_0^R dr\, r \int_{-1}^{+1} d\mu (1-\mu^2) \varphi(r,\mu) \frac{\partial \psi}{\partial \mu}$$

$$+ R^2 \int_0^{+1} d\mu\, \mu \varphi(R,\mu)\psi(R,\mu) + \int_0^R dr\, r^2 \int_{-1}^{+1} d\mu\, \psi(r,\mu)\Sigma_t(r)\varphi(r,\mu)$$

$$- \int_0^R dr\, r^2 \int_{-1}^{+1} d\mu\, \psi(r,\mu) \int_{-1}^{+1} d\mu' \Sigma_s(r,\mu' \to \mu)\varphi(r,\mu')$$

$$= \int_0^R dr\, r^2 \int_{-1}^{+1} d\mu\, \psi(r,\mu) S(r,\mu) - R^2 \int_{-1}^{0} d\mu\, \mu \varphi_0(R,\mu)\psi(R,\mu) \quad (4)$$

If a solution $\varphi(r,\mu) \in H_E$ to Eq.(4) is sought, and Eq.(4) is required to be valid for all $\psi(r,\mu) \in H_E$, the integral law corresponding to Eq.(1) is obtained :

Find $\varphi(r,\mu) \in H_E$
to Eq.(4) for all $\psi(r,\mu) \in H_E$.

The integral law is now in a form that is amenable to approximation by way of the finite element method. That is, rather than attempting to find a solution $\varphi(r,\mu)$ of Eq.(4) in the space of H_E, we seek the solution in a finite element subspace $S^h \subset H_E$. More specifically, we will seek a solution $\varphi^h(r,\mu) \in S^h$ such that Eq.(4) is satisfied for all $\psi^h(r,\mu) \in S^h$. Here, h is a parameter that depends on the mesh spacing to be used in the approximate solution ; S^h is a specially constructed subspace with basis functions

$$\psi_i^h(r,\mu), i = 1, 2, \ldots, N \quad ,$$

where N is the dimension of S^h, typically the number of nodes in the mesh. Thus, the integral law, Eq.(4) is replaced by an approximate integral law :

Find $\varphi^h(r,\mu) \in S^h$ *such that for all* $\psi^h(r,\mu) \in S^h$

$$- \int_0^R dr\, r^2 \int_{-1}^{+1} d\mu\, \mu \varphi^h(r,\mu) \frac{\partial \psi^h}{\partial r} - \int_0^R dr\, r \int_{-1}^{+1} d\mu (1-\mu^2) \varphi^h(r,\mu) \frac{\partial \psi^h}{\partial \mu}$$

$$+ R^2\int_0^{+1} d\mu\,\mu\,\varphi^h(R,\mu)\psi^h(R,\mu) + \int_0^R dr\,r^2\int_{-1}^{+1} d\mu\,\psi^h(r,\mu)\Sigma_t(r)\varphi^h(r,\mu)$$

$$- \int_0^R dr\,r^2\int_{-1}^{+1} d\mu\,\psi^h(r,\mu)\int_{-1}^{+1} d\mu'\,\Sigma_s(r,\mu'\to\mu)\varphi^h(r,\mu')$$

$$= \int_0^R dr\,r^2\int_{-1}^{+1} d\mu\,\psi^h(r,\mu)S(r,\mu) - R^2\int_{-1}^{0} d\mu\,\mu\,\varphi_0(R,\mu)\psi^h(R,\mu) \quad (5)$$

Since S^h is finite in dimension and $\varphi^h(r,\mu)\in S^h$, φ^h can be expanded as

$$\varphi^h(r,\mu) = \sum_{j=1}^{N} \phi_j \psi_j^h(r,\mu) ,$$

where ϕ_j=expansion coefficients,
ψ_j^h=basis functions.

If we substitute this expansion into Eq.(5) and require Eq.(5) to hold for all $\psi_i^h(r,\mu)$, $i=1,2,...,N$ to ensure that Eq.(5) is valid for all $\psi^h(r,\mu)\in S^h$, we obtain the matrix equation,

$$A\phi = S,$$

where

$$\phi = col(\phi_1,\phi_2,....,\phi_N)$$
$$S = col(S_1,S_2,....,S_N)$$
$$A = \{A_{ij}\}\ (N\times N \text{ matrix}),$$

and

$$A_{ij} = -\int_0^R dr\,r^2\int_{-1}^{+1} d\mu\,\mu\psi_j^h(r,\mu)\frac{\partial\psi_i^h(r,\mu)}{\partial r}$$

$$- \int_0^R dr\,r\int_{-1}^{+1} d\mu(1-\mu^2)\psi_j^h(r,\mu)\frac{\partial\psi_i^h(r,\mu)}{\partial\mu}$$

$$+ R^2\int_0^{+1} d\mu\,\mu\,\psi_i^h(R,\mu)\psi_j^h(R,\mu)$$

$$+ \int_0^R dr\,r^2\Sigma_t(r)\int_{-1}^{+1} d\mu\,\psi_i^h(r,\mu)\psi_j^h(r,\mu)$$

$$- \int_0^R dr\,r^2\int_{-1}^{+1} d\mu\,\psi_i^h(r,\mu)\int_{-1}^{+1} d\mu'\,\Sigma_s(r,\mu'\to\mu)\psi_j^h(r,\mu')$$

$$S_i = \int_0^R dr\,r^2\int_{-1}^{+1} d\mu\,\psi_i^h(r,\mu)S(r,\mu)$$

$$- R^2\int_{-1}^{0} d\mu\,\mu\,\psi_i^h(R,\mu)\varphi_0(R,\mu)$$

Finally we get a system of algebraic equations for the expansion coefficient ϕ_j, which can be easily evaluated by standard numerical methods.

3. Choice of Finite Elements

In genernal the finite element method is employed in a nodal fashion. That is, the expansion coefficients for the solution are nodal parameters that are typically the value of the solution or one of its derivatives at a node of the space angle mesh.[7]

In this study Lagrange interpolation polynomials are introduced over each local mesh or finite element. Linear or quadratic Lagrange polynomials are used as the basis functions in r and μ separately. Since the transport equation is only of first order, one can expect continuity of the angular flux at most. Therefore the use of Lagrangian elements that preserve continuity in the solution but not its derivatives would appear to be a proper choice for transport problems.[5] Lagrangian elements are formulated for multi-dimensional elements in terms of direct products of two or more one-dimensional Lagrangian basis functions.

The one-dimensional basis functions can be expressed as the standard tent functions[7] that are linear Lagrange polynomials as shown in Fig. 2. Higher order basis functions can also be defined over a general element as a direct product of higher order one-dimensional polynomials. To construct higher order elements, additional nodes are introduced and the higher order polynomials are defined over several nodes. This results in a coupling of nodes that would not be coupled by

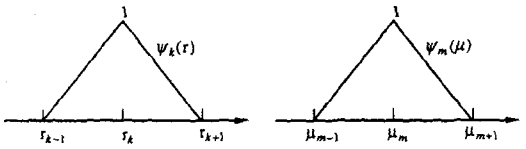

Fig. 2. Tent Finite Element Basis Functions

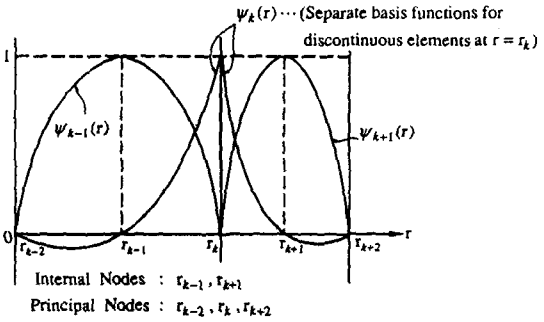

Fig. 3. Quadratic Lagrange Basis Functions

linear elements. This is not a concern with the angular elements because all nodes are coupled by scattering in any event. Fig. 3 illustrates a quadratic Lagrange polynomial[5,7] on a typical mesh interval and also indicates how discontinuous elements (in r and/or μ) are formulated by adding an additional principal node.

3.1. Discontinuous Angular Finite Elements

In curved geometry it is well known that the angular flux may be continuous as a function of the direction μ, and there is no discontinuity for $\mu=0$. Although the angular flux is continuous at $\mu=0$, its derivative with respect to μ will be discontinuous and the flux may change rapidly with μ near $\mu=0$. Moreover, such discontinuities in the angular derivative are present at points outside the material interface and for directions having $\mu>0$.[8] In order to consider such behavior in the angular flux with respect to μ, we can employ discontinuous angular finite elements.

The use of discontinuous angular finite elements is simply a matter of constructing basis functions, that are discontinuous at $\mu=0$, being careful to evaluate the integral in a piecewise fashion. This is easily accomplished by splitting the basis function at $\mu=0$ into two basis functions, one for $\mu=0^-$ and the other $\mu=0^+$. Thus there is a double node at $\mu=0$, as illustrated in Fig. 4 for a typical finite element mesh. Therefore the approximate solution is allowed to be discontinuous at $\mu=0$.

Since there exists the angular derivative in the transport term $\partial(1-\mu^2)\varphi/r\partial\mu$ in Eq.(1), integration must be performed carefully. The integration across the discontinuity will yield angular interface term which must be carefully incorporated into the integral law.

Let us consider in detail the angular redistribution term $\partial(1-\mu^2)\varphi/r\partial\mu$ sine no other terms are affected except for the spatial derivative in the transport term $\mu\partial r^2\varphi/r^2\partial r$, which is treated separately in Sec. III-2. As with the derivation of the original integral law, Eq.(4), it is multiplied by an arbitrary trial function $\psi(r,\mu)$ and integrate over the phase space, taking care to split up the integral to avoid the discontinuity in $\psi(r,\mu)$ at $\mu=0$:

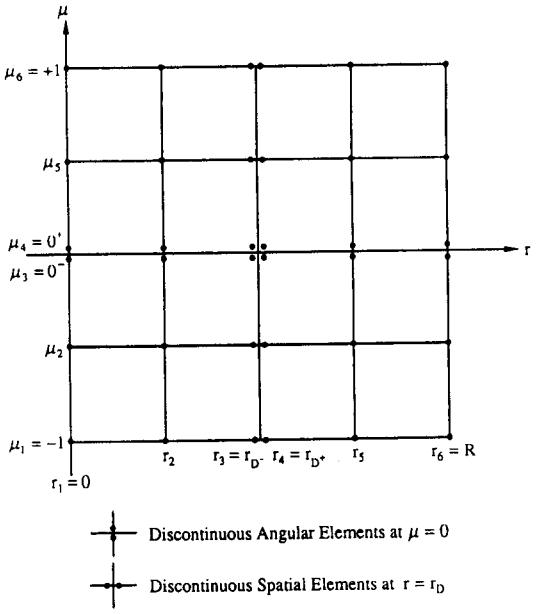

Fig. 4. Mesh Structure for Discontinuous Finite Elements

$$\int_0^R dr\, r\int_{-1}^{+1} d\mu\,\psi(r,\mu)\frac{\partial}{\partial\mu}\left[(1-\mu^2)\varphi(r,\mu)\right]$$

$$= -\int_0^R dr\, r\int_{-1}^{+1} d\mu\,(1-\mu^2)\varphi(r,\mu)\frac{\partial\psi(r,\mu)}{\partial\mu}$$

$$+\int_0^R dr\, r\left[\varphi(r,0^-)\psi(r,0^-) - \varphi(r,0^+)\psi(r,0^+)\right] \qquad (6)$$

The first term on the right side of Eq.(6) is identical to the original formulation and will not be modified, and the second term is angular interface term which is treated carefully.

As mentioned earlier, the angular flux may change rapidly with μ near $\mu=0$ for directions having $\mu>0$ at points outside the interface of material discontinuity. So this phenomenon can be viewed as the angular flux with respect to μ may vary abruptly at $\mu=0^+$ near material interface. Since the angular flux is analytically con-

tinuous in spite of the strong angular variations, the angular interface continuity condition is therefore assumed as

$$\varphi(r,0^+)=\varphi(r,0^-).$$

Thus the remaining angular interface term (AI) can be written as

$$AI = \int_0^R dr\, r\,\varphi(r,0^-)\left[\psi(r,0^-) - \psi(r,0^+)\right]$$

This term is additive to the integral law, Eq.(4), and results in the following matrix element:

$$AI_{ij} = \int_0^R dr\, r\,\psi_j^h(r,0^-)\left[\psi_i^h(r,0^-) - \psi_i^h(r,0^+)\right] .$$

which is additive to the matrix element A_{ij}.

3.2. Discontinuous Spatial Finite Elements

Although analytically the solution to the transport equation must be everywhere continuous in the spatial domain, there may be points at which the solution exhibits a near discontinuity. For example, the simple problem of a strong source of neutrons in a strong absorber surrounded by a vacuum will result in an angular flux with nearly discontinuous spatial dependence at the vacuum boundaries.[7] However it is difficult for the approximate solution to follow this discontinuous behavior because it is constrained to be continuous by the choice of the approximating subspace (Lagrange basis functions).

In order to allow the treatment of strong spatial variations in the flux, one can proceed as with the angular variable and simply construct discontinuous basis functions at the desired spatial positions, thus allowing the approximate solution to be discontinuous. However the presence of the spatial derivative in the transport term $\mu\partial r^2\varphi/r^2\partial r$ necessitates care when the transport equation is integrated over the spatial domain.

Let us consider a method for handling spatial discontinuity within the framework of the finite element scheme. We multiply spatial derivative term by an arbitrary function $\psi(r,\mu)$ and integrate the result over the phase space, allowing a discontinuity in the flux at $r=r_D$:

$$\int_0^R dr \int_{-1}^{+1} d\mu\,\psi(r,\mu)\mu\frac{\partial r^2\varphi(r,\mu)}{\partial r}$$

$$= -\int_0^R dr\, r^2\int_{-1}^{+1} d\mu\,\mu\,\varphi(r,\mu)\frac{\partial\psi(r,\mu)}{\partial r} + R^2\int_{-1}^{+1} d\mu\,\mu\,\varphi(R,\mu)\psi(R,\mu)$$

$$+ \int_{-1}^{+1} d\mu\,\mu\left[r_{D^-}^2\,\varphi(r_{D^-},\mu)\psi(r_{D^-},\mu) - r_{D^+}^2\,\varphi(r_{D^+},\mu)\psi(r_{D^+},\mu)\right] \quad (7)$$

Here we note that the right–hand side of Eq.(7) is identical to the original formulation except for the last term, which is defined as spatial interface term (SI). The next step is to use known information to reduce the SI term in a manner similar to the reduction of the boundary term by explicitly substituting the known boundary condition. Since the only known condition at an interface is that the solution $\varphi(r,\mu)$ at r_D is continuous, albeit strongly varying, let us use this condition in the direction of particle motion:

$$\varphi(r_{D^+},\mu) = \varphi(r_{D^-},\mu) , \quad \mu>0$$

$$\varphi(r_{D^-},\mu) = \varphi(r_{D^+},\mu) , \quad \mu<0 ,$$

we can get

$$SI = \int_{-1}^{0} d\mu\,\mu\,\varphi(r_{D^+},\mu)\left[r_{D^-}^2\,\psi(r_{D^-},\mu) - r_{D^+}^2\,\psi(r_{D^+},\mu)\right]$$

$$+ \int_0^{+1} d\mu\,\mu\,\varphi(r_{D^-},\mu)\left[r_{D^-}^2\,\psi(r_{D^-},\mu) - r_{D^+}^2\,\psi(r_{D^+},\mu)\right]$$

This term is also additive to the integral law, Eq.(4), and results in the following matrix element:

$$SI_{ij} = \int_{-1}^{0} d\mu\,\mu\,\psi_j^h(r_{D^+},\mu)\left[r_{D^-}^2\,\psi_i^h(r_{D^-},\mu) - r_{D^+}^2\,\psi_i^h(r_{D^+},\mu)\right]$$

$$+ \int_0^{+1} d\mu\,\mu\,\psi_j^h(r_{D^-},\mu)\left[r_{D^-}^2\,\psi_i^h(r_{D^-},\mu) - r_{D^+}^2\,\psi_i^h(r_{D^+},\mu)\right]$$

which is additive to the matrix element A_{ij}. Note that like an angular interface continuity condition this spatial interface continuity condition is included within the system of equations as a natural interface condition rather than the one imposed directly by the choice of the approximating subspace.

4. Numerical Results

The finite element methods discussed in the

preceding sections are applied to several typical problems in nuclear reactor analysis. The results of the two of these applications are presented next.

4.1. Critical Sphere Problem with Isotropic Scattering

The first application of our method is made to the classical eigenvalue problem of neutron transport theory–the calculation of the number of secondary neutrons, c, required per collision to achieve criticality in a sphere of given radius measured in mean free paths (mfp). The specific eigenvalue equation to be solved is

$$\frac{\mu}{r^2}\frac{\partial r^2\varphi(r,\mu)}{\partial r} + \frac{1}{r}\frac{\partial(1-\mu^2)\varphi(r,\mu)}{\partial\mu} + \varphi(r,\mu) = \frac{c}{2}\int_{-1}^{+1} d\mu'\varphi(r,\mu') \ ,$$

with boundary condition

$$\varphi(R,\mu) = 0 \ , \ \mu<0 \ ,$$

where R is the radius in mfp. Application of the finite element approximation developed in Sec. II results in the following generalized matrix eigenvalue problem.

$$A\phi = cM\phi, \qquad (8)$$

where **M** is the scattering matrix and **A** is the same as the matrix of coefficients given previously except that **M** has been substracted. Eq.(8) is solved using an power iteration method based on the Gaussian elimination algorithm and backsolving for each iteration until two successive values for c agreed to a desired precision.

All runs are performed with single precision (32–bit) arithmetic and the convergence criterion of the eigenvalue is chosen to be 10^{-6}, which is approaching the smallest round–off error realistically obtainable with single precision arithmetic.

Four different size of spheres are analyzed with various order of finite elements and mesh spacings. Continuous finite elements in space and angle are used for all runs, and uniform spatial and angular meshes are used. Table 1 summarizes the results for the four spheres and includes benchmark eigenvalues reported by Kaper et al.,[9] for the different size of spheres.

As is seen in Table 1, the accuracy of the eigenvalue decreases as the number of meshes increases. The reason for this is that the size of matrix **A** in Eq.(8) becomes larger as the number

Table 1. Number of Secondary Neutrons per Collison for Criticality in Spherical Geometry with Isotropic Scattering

Radius (mfp)	Benchmark[a] (Ref. 9)	LL[b](2, 2)	LL(4, 4)	LL(6, 6)	QQ[b](4, 4)	QQ(8, 8)
2.0	1.395872	1.394893 (0.070%)[c]	1.398715 (0.204%)	1.398943 (0.220%)	1.402499 (0.475%)	1.404664 (0.630%)
4.0	1.138460	1.138878 (0.037%)	1.139633 (0.103%)	1.139718 (0.111%)	1.141127 (0.234%)	1.141887 (0.301%)
10.0	1.028149	1.028297 (0.014%)	1.028423 (0.027%)	1.028443 (0.029%)	1.028737 (0.057%)	1.028830 (0.066%)
20.0	1.007628	1.007737 (0.011%)	1.007750 (0.012%)	1.007754 (0.013)	1.007796 (0.017%)	1.007756 (0.013%)

[a]Original results have been rounded off to seven significant figures

[b]L = linear, Q = quadratic ; spatial element first ; number of mesh intervals in each direction with spatial mesh first

[c]Relative errors in percent

Table 2. Scalar Flux Results in a Critical Sphere for Radius R=10.0 mfp

Position (mfp)	Benchmark[a] (Ref. 9)	LL[b](4, 4)	LL(8, 8)	QQ[b](4, 4)	QQ(8, 8)
0.0	1.0[c]	1.0	1.0	1.0	1.0
2.5	0.91245	0.90324 (1.01%)[d]	0.90875 (0.40%)	0.93057 (1.99%)	0.92874 (1.79%)
5.0	0.67710	0.66800 (1.34%)	0.67227 (0.71%)	0.67983 (0.40%)	0.68527 (1.21%)
7.5	0.36565	0.35212 (3.70%)	0.36161 (1.11%)	0.35990 (1.57%)	0.36797 (0.64%)
10.0	0.05570	0.05576 (0.11%)	0.05783 (3.85%)	0.06072 (9.01%)	0.06121 (9.90%)

[a]Original results have been rounded off to six significant figures

[b]Same notation as Table 1

[c]All center fluxes are normalized to unity

[d]Relative errors in percent

of meshes increases, hence the spatial accuracy using finer mesh seems to be decreased by the accumulation of round-off error resulted from the significantly increased number of operations during the Gaussian elimination. Another point is that the results using the quadratic elements are poorer than those of the linear elements. This is because the matrix **A** in Eq.(8) is a banded matrix. The use of quadratic elements for the basis functions results in a coupling of nodes that would not be coupled by linear elements. Therefore the bandwidth of the matrix **A** by using the quadratic elements is wider than that by the linear elements. In the Gaussian elimination process, the number of multiplication and divisional operations of a wide bandwidth matrix is obviously more than that of a narrow bandwidth matrix, hence round-off error becomes larger in a wide bandwidth matrix.

Table 2 contains the nodal scalar fluxes corresponding to the eigenfunctions for the sphere of radius 10.0 mfp. The results are tabulated for various mesh spacings and finite elements. Again, these scalar flux values are compared with the benchmark values from Ref. 9. On the basis of the eigenvalue results, less accurate results are obtained for the scalar flux. However, the comparison should somewhat inexact due to the normalization used (flux at center of sphere=1.0) to compare with the benchmark results.

4.2. Multi-Region Problem with Strong Heterogeneities

The finite element method is applied to a multi-region problem with strong material discontinuities and source discontinuities as shown in Fig. 5. In this problem, discontinuous linear finite elements are utilized in both space and angle.

The spatial region is subdivided into 40 equally spaced mesh intervals and has one additional node at each material interfaces. The angular domain consists of a uniform mesh of 4 intervals and has one additional node at $\mu=0$. Therefore the simultaneous set of linear algebraic equations which has 44×6 unknowns are set up. Hence the system of equations can be solved directly by the use of the Gaussian eliminaton technique.

The scalar flux distribution of the above calculation is shown in Fig. 6 compared with that obtained from the one-dimensional discrete ordin-

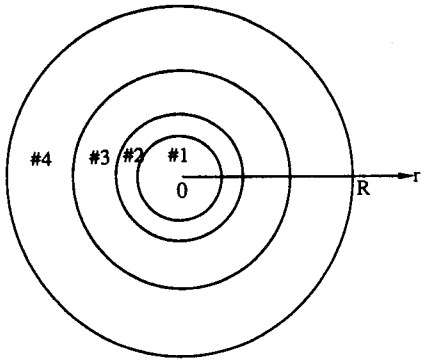

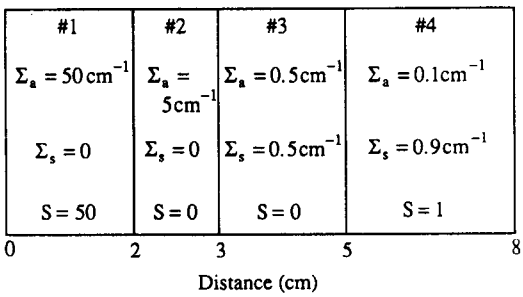

Fig. 5. Physical Configuration for Multi-Region Problem

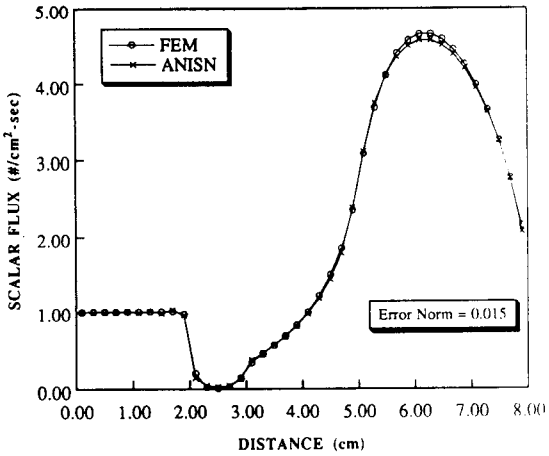

Fig. 6. Comparison of Results from ANISN Code and FEM for Cell Centered Scalar Fluxes for Multi-Region Problem Described in Fig. 5

ates code, ANISN[10]. In ANISN calculation 40 equally spaced mesh intervals and 9 angular directions are used. To quantify the discrepancy between the result of the finite element method and that of the ANISN code calculation in the heterogeneous problem, we introduce the following error norm defined by

$$|\Phi| = \frac{\left|\sum_i (\Phi_i - \Phi_i^{ANISN})\right|}{\left|\sum_i \Phi_i^{ANISN}\right|}, \quad i = 1, 2, \ldots, I.$$

Here, Φ^{ANISN} is the ANISN solution, while Φ is the calculated cell centered scalar flux.

5. Conclusions

Based on the results, the following conclusions can be made concerning the application of the finite element method to the numerical solutions of the one-dimensional transport equation in a spherical geometry.

1) For criticality calculations, the results of the finite element method by using the linear finite elements are better than those obtained by the quadratic finite elements.
2) The finite element method is capable of treating problems with strong material discontinuities when discontinuous angular and spatial elements are used.
3) The main difficulty in handling the finite element method is to store the coefficient matrix and to solve the corresponding set of equations directly, at least for the first-order approach. For large problems, especially multi-dimensional applications, the storage requirement can be an obstacle to many computing installations.

In summary, the finite element method can be considered as a viable and competitive metod for solving the one-dimensional transport equation in spherical geometry when it is applied to the first-order form of the transport equation using the Galerkin principle.

References

1. J. Pitkäranta and P. Silvennoinen, "Finite Element Analysis of Some Critical Fast Assemblies," *Nucl. Sci. Eng.*, **52**, 447 (1973).
2. W.F. Miller, Jr., E.E. Lewis, and E.C. Rossow, "The Application of Phase-Space Finite Elements to the One-Dimensional Neutron Transport Equation," *Nucl. Sci. Eng.*, **51**, 148 (1973).
3. W.F. Miller, Jr., E.E. Lewis, and E.C. Rossow, "The Application of Phase-Space Finite Elements to the Two-Dimensional Neutron Transport Equation in X-Y Geometry," *Nucl. Sci. Eng.*, **52**, 12 (1973).
4. S. Ukai, "Solution of Multi-Dimensional Neutron Transport Equation by Finite Element Method," *J. Nucl. Sci. Tech.*, **9**, 366 (1972).
5. W.R. Martin and J.J. Duderstadt, "Finite Element Solutions of the Neutron Transport Equation with Applications to Strong Heterogeneities," *Nucl. Sci. Eng.*, **62**, 371 (1977).
6. E.E. Lewis and W.F. Miller, Jr., "Computational Methods of Neutron Transport," Chap. 1 and 3, John Wiley & Sons, New York (1984).
7. J.J. Duderstadt and W.R. Martin, "Transport Theory," Chap. 8, John Wiley & Sons, New York (1979).
8. G.I. Bell and S. Glasstone, "Nuclear Reactor Theory," Chap. 3 and 5, Van Nostrand Reinhold Co., New York (1970).
9. H.G. Kaper, A.J. Lindeman, and G.K. Leaf, "Benchmark Values for the Slab and Sphere Criticality Problem in One-Group Neutron Transport Theory," *Nucl. Sci. Eng.*, **54**, 94 (1974).
10. "ANISN-ORNL, A One-Dimensional Discrete Ordinates Transport Code System with Anisotropic Scattering," CCC-254, Oak Ridge National Laboratory, 1973.